Published in final edited form as:
*Electroanalysis*. 2013 December ; 25(12): 2586–2594. doi:10.1002/elan.201300349.

# Lab-on-a-Chip Sensor with Evaporated Bismuth Film Electrode for Anodic Stripping Voltammetry of Zinc

**Wenjing Kang**[a], **Xing Pei**[a], **Wei Yue**[b], **Adam Bange**[c], **William R. Heineman**[b], and **Ian Papautsky**[*,a]

[a]BioMicroSystems Lab, Department of Electrical Engineering and Computing Systems, University Of Cincinnati, Cincinnati, OH, 45221 tel.: (513) 556-2347; fax: (513) 556-7326

[b]Department of Chemistry, University of Cincinnati, Cincinnati, OH 45221

[c]Department of Chemistry, Xavier University, Cincinnati, OH, Cincinnati, OH 45221

## Abstract

In this work, we report on the development of a lab-on-a-chip electrochemical sensor that uses an evaporated bismuth electrode to detect zinc using square wave anodic stripping voltammetry. The microscale electrochemical cell consists of a bismuth working electrode, an integrated silver/silver chloride reference electrode, and a gold auxiliary electrode. The sensor demonstrated linear response in 0.1 M acetate buffer at pH 6 with zinc concentrations ranging from 1 μM to 30 μM and a calculated detection limit of 60 nM. The sensor was also able to successfully detect zinc in a bovine serum extract and the results were verified with independent AAS measurements. These results demonstrate the advantageous qualities of this lab-on-a-chip electrochemical sensor for clinical applications, which include a small sample volume (μL scale), reduced cost, short response time and high accuracy at low concentrations of analyte.

## 1 Introduction

Zinc (Zn) is an essential trace element that plays a critical role in human metabolic and immune systems [1–6]. Abnormally-low levels of Zn are often associated with inflammation and infection [7–9]. While Zn homeostasis can be easily restored though Zn supplementation [10–13], overdosing is a serious threat that can lead to copper deficiency and neurologic disease such as myelopathy or Alzheimer's [6,14,15]. Thus, constant monitoring of Zn levels in patient's blood becomes of critical importance for the supplementation strategy to work. Traditionally, such measurements are performed in blood serum with total Zn concentrations in the 65 to 95 μg/dL (9.9 to 14.5 μM) range [16], using conventional methods such as atomic absorption spectroscopy (AAS) [17,18] and inductively coupled plasma mass spectrometry (ICP-MS) [19,20]. Both of these methods provide accurate measurements in diluted serum or blood, but require bulky and expensive instruments and specialized personnel to operate them. Furthermore, shipping of samples to a centralized lab can present significant time delays of potentially time-sensitive information. Due to these challenges, conventional methods are not suitable for bed-side monitoring of Zn levels in blood for some patients in medical applications, and thus, a simple and low-cost instrument with rapid response is in great demand.

Compared with spectroscopic methods, anodic stripping voltammetry (ASV) rises as a promising alternative for measurements of trace metals such as zinc, lead and cadmium



[*]ian.papautsky@uc.edu.

[21,22]. This technique is more time-and-cost-effective while providing limits of detection (*LOD*) in the sub-nanomolar range. Previous work has been mainly based on mercury electrodes because of the stable performance and low detection limits [23–26], but handling and disposal issues stemming from mercury toxicity now impede widespread application.

Bismuth (Bi) has been gaining popularity in recent years as an alternative electrode material for electrochemical measurements. It forms low-temperature alloys with heavy metals to enable preconcentration and offers a wide negative potential window. Most importantly it is much less toxic than mercury and is environmentally-friendly [27]. Wang et al.[28] and Guo et al.[29] compared performance of in situ deposited Bi films on carbon-based electrodes to mercury film electrodes (MFE) for ppb level Zn measurements in acetate buffer and found responses to be comparable. Kefala et al.[30,31] used in situ and ex situ deposited Bi with or without the presence of Nafion coating on glassy carbon electrode, and achieved a sub-ppb (nM) detection limit for Zn.

Still, detection of Zn in complex sample matrices such as serum or whole blood by ASV remains challenging. Direct measurement of Zn in serum is not possible because some Zn is bound to protein and will not appear upon analysis. Thus an acid-digestion procedure must be used to break up protein and release Zn into the aqueous phase [32]. Kruusma et al.[33] reported an extraction procedure to reduce or even remove the organic components and facilitate electrochemical measurements. Wei et al.[34] developed an improved extraction procedure for stripping analysis that achieves 97% recovery of Zn. This approach enabled us to accurately detect concentrations of Zn in bovine serum and has the potential to be a viable technique for human serum or blood.

To overcome shortcomings of the existing Bi electrodes, we developed a miniaturized lab-on-a-chip sensor with electrodeposited Bi thin film electrode for measuring Zn. Our sensor size is approximately 15 mm×19 mm, requires only microliters of sample, and performs analysis in less than 15 min. These features make it ideal for point-of-care applications. The sensor consists of a gold auxiliary electrode (AE), a silver/silver chloride (Ag/ AgCl) reference electrode (RE) and a bismuth working electrode (WE). The layout of electrode patterns was generally akin to our earlier work [35] with adjustment of the connection pads. Meanwhile we developed a user-friendly interface that integrated an edge board connector and a mini-USB port to provide simplified connection and accessibility [36]. The sensor was fabricated following a series of photolithography, wet etching, evaporation, lift-off, and electroplating procedures. In this work, we focused on measurement of Zn and achieved a 60 nM (3.9 ppb) (calculated by $3\sigma$/slope) LOD in 0.1 M, pH 6 sodium acetate buffer. We also demonstrated successful measurement of approximately 4 μM Zn in extracted bovine serum using the standard addition method and confirmed the result by separate AAS measurements.

## 2 Experimental

### 2.1 Reagents

Reagents were purchased from commercial vendors. Piranha solution was prepared from 7 $H_2SO_4$:3 $H_2O_2$ (volume ratio) to clean glass substrates. Two types of wet etchants were used to obtain electrode patterns: gold etchant was made from 20 g $I_2$ :5 g KI:200 mL de-ionized (DI) water (w/w/v); titanium etchant was made from $HNO_3$ :2 HF:7 DI water (volume ratio. The salts – $I_2$, KI –and acids – $HNO_3$ and HF – were purchased from Fisher Scientific. Bismuth target (Bi pieces, 1–12 mm, 99.999% trace metal basis) was purchased from Sigma Aldrich. We purchased silver plating solution (Silver Cyless II 10.00 GM per 1.00 GL) from Technic Inc., and zinc stock solution (Zinc Standard for AAS, 1000 mg/L in 2% nitric acid, Fluka) from Sigma Aldrich. A 1 M KCl solution was prepared from salt (Fisher Scientific)

and used to chloridize the Ag reference electrode into Ag/AgCl. Acetate buffer (pH 4.65, 0.1 M) was purchased from Fluka and adjusted to pH 6 with NaOH and acetic acid (Fisher Scientific). Hyclone Characterized Fetal Bovine Serum from Thermo Scientific was used for the serum extraction procedures.

### 2.2 Serum Extraction

First, 10 mL (5 mM) dithizone in chloroform was deprotonated by mixing with 10 mL (pH 9) 1 M ammonia/ 0.5 M ammonium buffer solution. Then the deprotonated form of dithizone was mixed with the solution containing serum and 0.5 mL of 0.05 M potassium thiocyanate in ethanol, followed by sonication for a period of 5 min. Afterward, the solution was transferred into a 50 mL plastic tube and centrifuged for 10 min at a rate of 4000 rpm to separate the two phases. The organic phase was collected and sonicated with 10 mL of 1 M sulfuric acid for another 5 min. After extraction procedures, we adjusted the pH of the sample to 6 using NaOH and diluted the sample with pH 6, 0.1 M acetate buffer by a factor of 2.

### 2.3 Device Design and Fabrication

The steps for fabrication of the electrochemical sensor varied, depending on the type of Bi film used for WE. The electrodeposited Bi WE process included a single evaporation step to deposit gold metal layer, followed by a single photolithography patterning step and electrode-position of Bi (Figure 1a). The evaporated Bi WE process included the first evaporation step to deposit gold metal layer, the first photolithography patterning step to define electrode shape, second photolithography step to define sacrificial resist mask, a second e-beam evaporation step to deposit a thin film of bismuth, and a lift-off process to pattern Bi WE (Figure 1b).

Glass slides (3 in squares, 0.028 in thick, S. I. Howard Glass Co., Inc.) were cleaned using piranha solution, and coated by layer of 20 nm titanium and 200 nm gold using e-beam evaporation. Gold electrode patterns were created using photolithography (Shipley 1818 resist), followed by wet etching. For the evaporated Bi film electrodes only, a second photolithography step was used to create a thick sacrificial mask of photoresist, followed by a second evaporation step to deposit 200 nm layer of bismuth. This bismuth film was patterned using a lift-off process to achieve clean bismuth working electrodes, as shown in Figure 1b. To fabricate the polydimethylsiloxane (PDMS, Sylgard 184, Dow Corning) well, we used standard soft lithography and plasma bonding techniques (plasma surface treater, BD-20AC, Electo-Technic Products Inc.).

All electrodeposition steps were performed after PDMS wells were bonded to glass substrates and cured. To form Ag/AgCl reference electrode [32], chronopotentiometry was first used to electrodeposit a thin layer of silver by the reduction of silver ion using 3 mA/ $cm^2$ current density for 60 s. This was followed by a second step where silver was oxidized in the presence of chloride ion for 30 s, thus depositing silver chloride on half of the electrode. Electrodeposition of the Bi film was carried out using chronoamperometry at −0.8 V for 240 s followed by rinsing with DI water for 60 s. Figure 1c shows a close-up view of a completed sensor with all the electrodes indicated.

### 2.4 Procedure

A miniature USB Potentiostat (WaveNow, Pine Instruments, Inc.) was connected to a computer and also to an interface connector with an electrochemical cell inserted. Figure 1d demonstrates the PCB-based edge board connector interface with a sensor inserted, where the interface was connected to the potentiostat via a mini USB cable. We used 100 μL as the sample volume for all the experiments in acetate buffer. With cyclic voltammetry (CV) in

pH 4.65, 0.1 M acetate buffer, the potential window of an evaporated bismuth WE was confirmed to be similar to that of an electroplated bismuth electrode. Based on previous optimization of ASV conditions in pH 6 0.1 M acetate buffer [36], we used the following parameters: −1.6 V as preconcentration potential with 600 s duration, stripping range from −1.6 V to −0.6 V, and waveform parameters of 70 ms for period, 4 mV for increment and 25 mV for amplitude. Zn concentrations from 1 μM to 30 μM in acetate buffer were used to construct the calibration curve.

For the detection of unknown Zn level in extracted bovine serum, we increased the sample volume to 200 μL and adjusted stripping parameters based on further optimization in serum extract to be −1.4 V for preconcentration potential, 900 s for duration, and 40 ms for period. Also, we introduced a surface preconditioning process before deposition to eliminate possible variations between each measurement, including four segments of CV scanning from −1.2 V to −0.4 V in the serum sample. We used the method of standard additions to determine the actual concentration of Zn in extracted serum.

## 3 Results and Discussion

### 3.1 Bismuth Film Electrodes

We carefully examined electrodeposition of Bi films to improve sensor performance in biological samples. In our earlier work, we electrodeposited the Bi WE at −0.8 V with agitation of the deposition solution for 240 s. The Bi film was approximately 160 nm thick with surface roughness of 230±49 nm [35]. As demonstrated in Figures 2a and d, the rough Bi film suffered from severe crystallization which leads to poor coverage of most areas of the gold substrate; the film is thicker at the edge than the center of the circular electrode and has branches extending towards the RE, which causes huge variations in Zn accumulation on the WE during the deposition step because of surface area variability. When this Bi film was tested for ASV of Zn in sodium acetate buffer, it exhibited high *LOD*, which was calculated to be 6 μM, and it could only provide measurements in serum samples spiked with 20–60 μM of Zn.

To reduce surface roughness of the Bi films and improve repeatability of the sensor, we optimized the fabrication procedures as reported by Pei et al. [36]. While it is a common practice to stir solution during electrodeposition to minimize mass transport limitations, we found that using quiescent solution [37] yielded bismuth films with smoother surfaces and cleaner edges, reducing the formation of long branches which might short circuit the closely placed WE and RE. We de-oxygenated the bismuth plating solution [38,39] to increase the film thickness to about 200 nm and achieve better film quality. As shown in Figures 2b and e, the improved electroplated film completely covers the Au surface, and the surface is smoother and softer than those in a and d with less Bi crystals on the center. However, Bi still tended to aggregate along the rim, forming extra mesh-like membranes that extended into the gap between WE and RE. Thus the surface roughness was still not favorable, calculated as 132±98 nm; the large standard deviation revealed huge differences in surface morphologies between the center and the thick and rough rim area. The variations of Bi surface still introduced large uncertainty into the voltammograms in acetate buffer, and the inability to directly measure Zn levels in serum was not solved by this strategy.

To further improve the film quality, we evaporated bismuth on gold, which was expected to yield films of the highest quality possible. Electrode patterns were formed by lift-off to guarantee a clean edge for the WE. As demonstrated in Figures 2c and f, evaporated Bi electrodes offer a significant improvement over the earlier electro-deposited Bi electrodes. The Au surface was evenly covered by about 300 nm of Bi film with hardly any defects and the surface roughness was greatly reduced to 40 ± 2 nm. Also the shape and location of the

Bi film was precisely matched to the Au pattern. Consequently, the electrode performance improved significantly. The variation of performance in buffer was reduced and acceptable results could now be achieved in serum matrix.

To demonstrate the overall improvement of the evaporated Bi electrode, we compared the performances of the three types of Bi WE with ASV determinations of Zn. Figure 2g shows the Zn stripping peak current and reproducibility for electrodes fabricated using these different approaches. Compared to the results from the first generation of electroplated bismuth film in the left column, the improved bismuth electroplating procedures created finer and neater films, which caused a minor increase in the Zn peak current from 13 μA to 14.5 μA and a dramatic decrease in coefficient of variation from 42% to 8% as shown in the middle column. After we used e-beam evaporation to deposit the Bi film, the peak amplitude of the signal current dropped from 14.5 μA to ~12 μA due to the large decrease in film roughness which is related to the electrode surface area, while the variation was minimized to less than 2% as shown in the right column.

### 3.2 Calibration of Evaporated Bismuth Electrodes in pH 6 Acetate Buffer

We first used cyclic voltammetry (CV) to confirm the potential window of our Bi electrode. Voltammograms in pH 4.65 acetate buffer showed a flat region from −0.3 V to −1. 4 V, which agrees with our previous results [36] as well as others [28]. Next, to construct a calibration plot, square wave ASV (SWASV) of zinc was performed in the concatenation range of 1 μM to 30 μM in acetate buffer. We used SWASV parameters listed in the experimental section which are the same for electroplated Bi electrode. For most concentrations, we repeated experiments three times ($n$=3) using a new disposable device each time to obtain standard deviation. For 1 μM, which was the lowest Zn concentration sample, an $n$=5 was used to calculate the detection limit based on 3$\sigma$/slope.

This Bi WE was successfully calibrated in 0.1 M pH 6 acetate buffer, and the voltammograms were compared with electroplated Bi WE. The voltammograms in Figure 3a show the Zn stripping peak at around −1250 mV for higher concentrations, but shifting positively with decreasing Zn levels. One possible reason for this is that oxidation of the first monolayer of Zn that is deposited directly on Bi requires larger energy than stripping of subsequent layers of Zn that have deposited on Zn. However, the differences are not sufficient to cause double stripping peaks. Consequently, Zn stripping peaks in the 10 μM to 30 μM range exhibit shoulders on the positive side which broaden the peaks. As Zn levels decrease, Zn atoms stripping from Bi surface become the primary source, thus the peaks gradually migrated to nearly − 1.1 V [40–42]. Also, the Zn stripping peaks are ~100 mV more positive than those on electroplated Bi electrodes [32]. This shift might be attributed to the different sequences of fabricating the reference electrodes, in that Ag/AgCl RE electroplating was the last step before the predeposition step for sensors with evaporated Bi, while Ag/AgCl was plated one step prior to the electroplating of Bi before predeposition for sensors with electroplated Bi WE. The inevitable variations involved in the soaking and rinsing steps could potentially shift the half-cell potential of the reference electrode by altering the composition of the Ag/AgCl layer to a certain extent, resulting in shifted Zn peaks.

A calibration plot was constructed based on Zn peak heights versus concentration, and then detection limit was calculated. The curve in Figure 3b shows a favorable linear relationship between peak height of stripping current and Zn concentration; the correlation equation was $I$(μA)=0.5782×[Zn(μM)]−0.4192 ($R^2$=0.99 for $n$=7). The *LOD* was calculated to be 60 nM, exhibiting a 100× improvement over the electroplated Bi WE [32] despite the decrease in sensitivity from 1.48 μA/μM to 0.58 μA/ μM. This substantial improvement is due to the more precise process control of the evaporation technique, which allowed us to create

smoother films with identical shapes on the structural layer, thus minimizing variation of surface roughness, actual surface areas and shapes of the Bi film. As a result, we achieved enhanced reproducibility and lowered *LOD*.

### 3.3 Optimization of ASV Parameters in Extracted Serum

Further adjustments were necessary for application of the Bi WE in serum matrix since the behavior was quite different from acetate buffer. Initially we did several measurements in 100 μL of extracted serum diluted one time by acetate buffer, using the same parameters as optimized in acetate buffer. Bubbles formed on the working electrode surface during deposition at −1.6 V, which disrupted Zn deposition by blocking the solution from the electrode surface. The resulting voltammograms were not analytically useful, as Zn peaks were distorted and somewhat obscured by a large $H^+$ reduction wave leading to poor reproducibility.

To remedy this, we optimized the voltammetry parameters starting by examining a series of deposition potentials: −1.6 V, −1.5 V, −1.4 V and −1.3 V. For −1.6 V, the $H^+$ reduction current was the highest but variability was the largest. While signal was almost the same for the rest of the tested potentials, depositions at −1.3 V and −1.5 V exhibited larger variability in Zn peaks. Thus, we chose −1.4 V deposition potential, which was sufficiently negative to efficiently deposit Zn, but not too negative to introduce large $H^+$ reduction current. Figure 4a shows Zn stripping current amplitudes and variations for each potential, indicating that −1.3 V, −1.4 V and −1.5 V could all be considered, but −1.4 V was preferred for its stability.

Different preconcentration times were also examined, as illustrated in Figure 4b. The peak current for Zn stripping increased rapidly with deposition time for the first 600 s before plateauing at 900 s. Although 600 s deposition provided adequate signal current, we selected 900 s due to the improved stability and consistency in the voltammograms despite a negligible drop in Zn peak amplitude. The 900 s accumulation may seem long, especially compared with 60–120 s typically reported in literature. This is due to the limited agitation in the electrochemical cell, and thus poor mass transport of metal ions to the electrode surface. While we are using a vibrating platform to agitate sample inside our small electrochemical cell, the resulting mass transport is not nearly as efficient as in bulk, stirred samples. In essence, our analysis is in performed a nearly-quiescent state, which limits mass transport and necessitates a longer preconcentration time.

In conjunction with deposition time, we examined sample volume used in our electrochemical cell. The results show that the stripping peak current is not proportional to sample volume (Figure 4c). While at first glance this maybe surprising, the results in Figure 4c are consistent with the mass-transport limitations of our system. For the 50, 100, and 200 μL samples, the height of liquid in a 4.5 mm radius PDMS well is 0.79, 1.57, and 3.14 mm, respectively. Neglecting any convection and considering the sample as quiescent, we can calculate the diffusion length for $Zn^{2+}$ ions in each sample. The diffusion length $\delta_D$ is given as $\delta_D = (Dt)^{1/2}$, where $D$ is the diffusion coefficient of $Zn^{2+}$ ions in electrolyte, and $t$ is deposition time. From literature, diffusion coefficient can be estimated as $D=10^{-9}$ $m^2/s$ [43]. Using $t$=600 s, the diffusion length can be approximated as $\delta_D$ = 0.77 mm. Considering that height of liquid layer is nearly the same as the diffusion length for the 50 μL sample, nearly all of the $Zn^{2+}$ ions must accumulate on the electrode surface. Increasing height of the liquid layer (e.g. increasing sample volume to 100 μL and 200 μL) does not increase peak current since diffusion length cannot extend that far, so the additional sample volume is not accessible to the electrode. As a result, data in Figure 4c do not show a substantial change in signal from 50 μL to 200 μL sample volume. While in this work we used a 200 μL sample volume for all experiments, due to a minute increase in peak current, it remains possible to

reduce the sample volume down to 50 μL in future applications without sacrificing signal strength.

We used a CV-based preconditioning process within the stripping range of Zn for Bi WE to achieve better reproducibility. Although we found evaporated Bi films to be thicker and to have less surface roughness than electroplated films, they occasionally produced abnormally low currents at relatively high concentrations of Zn, indicating that the Bi films exhibited some device to device variation. This variability may have been due to the intermetallic interaction between Bi and Zn, where small differences in the surface produce large variations in Zn deposition. We found that the CV pretreatment of the electrode alleviated this problem to some extent. Others [44–46] have also used this approach to achieve enhanced electron transfer, higher sensitivity, and more stable performance. Our adopted procedure consisted of scanning cyclic voltammetry from −1.2 V to −0.4 V at 100 mV/ s sweep rate for four segments in serum sample before the preconcentration step. This step allowed the surface to equilibrate to the conditions that we used for our analysis, and the voltammograms then remained flat around the Zn stripping potential. After preconditioning, we observed more stabilized stripping curves and smaller variations among different runs of our experiments.

### 3.4 Zinc Detection in Extracted Serum

To demonstrate sensor operation with biological samples, unknown Zn concentrations were detected in bovine serum extracts using the method of standard additions on pretreated Bi WE (Figure 5). These Zn peaks broadened from 300 mV to approximately 500 mV, due to changes in sample composition such as the residual organic components, increased sample viscosity, and decreased ionic strength. An approximately 50 mV positive migration of Zn peaks was observed as concentrations decreased from 5 μM to 1 μM, which is also the trend observed in acetate buffer. A similar trend was observed by us using electroplated Bi electrodes [32].

The Zn peaks in serum appear to shift from −1250 mV to a more positive potential of approximately −750 mV, when compared with stripping in acetate buffer. This is shown in Figure 5c. The major reason for this shift is the several orders of magnitude difference in the chloride concentration between the two sample matrices. The chloride concentration in serum may vary, but generally remains in the 96–106 mM range [47]. The acetate buffer, on the other hand, has little chloride, primarily arising from the impurity of the sodium hydroxide salt used to adjust the pH (0.001% from Certificate of Actual Lot Analysis, or $4.7\times10^{-7}$ M calculated based on the amount of sodium hydroxide added for the pH adjustment). Another possible source could be $Cl^-$ dissolved from the naked Ag/AgCl RE, but since the deposition time in acetate buffer is only 10 min, it is not possible for the dissolution of AgCl to reach equilibrium. Thus, the impurity in NaOH is the main source of chloride in the acetate buffer. Using the Nernst equation, the difference in RE potential between serum and buffer due to chloride ion concentration is calculated to be ~300 mV, which is the majority of the observed positive shift in Figure 5c. This also suggests that it may be feasible to shift the Zn peaks in acetate buffer to the same potential as in serum extract by adding $Cl^-$ to the buffer. Manually shifting the voltammograms obtained in acetate buffer by 300 mV positively, as indicated in Figure 5c, we can observe the overlapping background currents of the two sample matrices.

The reason for the additional ~150 mV shift of Zn peaks remains unclear, but we can tell from the voltammograms that it is related to the changes of the RE surface in the serum extract. Further examination of the RE changes in different matrices and following sample preparation procedures is needed, since the electrodes are unprotected in the sample. Nevertheless, this uncertainty is rather stable because the voltammograms based on multiple

repetitions of measurements at each data point are consistent. Furthermore, this shift does not actually affect our ability to detect Zn since we are measuring amplitude of the Zn peak current, and the Zn peak potentials do not exhibit direct correlations to the peak amplitudes.

Due to complexity of serum as biological sample, it is possible for other trace metals to interfere with anodic stripping of Zn. The metals that exhibit stripping peaks in the potential range similar to Zn include Mn, Cr, and Cd. Other metals present in serum, such as Cu or Pb, strip at more positive potentials and are not expected to interfere. The Cd and Mn peaks are expected to occur at ~400 mV more positive or 200 mV more negative than Zn, respectively. These stripping peaks, however, are absent from the voltammograms. Cr is present in trace levels in serum, approximately 77–500 nM (4–27 ppb) [48]. These trace levels are at the *LOD* of our sensor, and thus any presence in the sample would lead to minute peaks that would not severely affect Zn stripping. Thus, any interference by other trace metals can be neglected.

The method of standard addition was used to determine unknown Zn concentrations in serum samples. The resulting calibration curve in Figure 5b showed high linearity (~97%) and sensitivity (0.13 μA/μM), indicating good sensing performance in serum. Zn concentration was determined to be 3.9 μM (260 ppb or 26 μg/dL) from the intercept of the plot in Figure 5b, which was in close agreement with an independent AAS measurement of 4.5 μM. Thus, the Bi WE exhibits the capability to measure Zn at much lower concentrations than the ~20 μM result reported previously by Kruusma et al. [49] using boron-doped diamond or by Kumar et al. [50] who used a hanging mercury drop electrode (HMDE) for measurements in the range of 49 μM–63 μM. ICP-MS techniques have been reported to detect Zn with a LOD of ~61 nM (4 ppb) in whole blood or serum by Barany et al. [20]. Although our miniaturized voltammetric sensors are currently unable to match the precision and limits of detection of modern spectroscopic and mass spectrometry techniques, the measurements that they are able to do are still in the physiologically relevant range, and they can potentially be used for rapid, inexpensive, point-of-care analyses.

## 4 Conclusions

In this work, we presented a microfabricated electrochemical cell for point-of-care measurements with an evaporated bismuth working electrode, a silver/silver chloride reference electrode and a gold auxiliary electrode. The analysis time required takes 10–15 min for each measurement, which is greatly reduced compared with AAS or ICP-MS. With improved film consistency and quality, the evaporated Bi WE provides favorable reproducibility and sensitivity for detection of zinc in 100 μL acetate buffer with calculated LOD of 60 nM (3.9 ppb). The sensor performance was also confirmed by AAS.

The capability to detect Zn concentrations in microliter sample volumes offers an alternative to the conventional methods and can be applied in situations where sample volume is limited. The size of the sensor is 15 mm × 19 mm and provides a convenient connection to a portable potentiostat, which is suitable for various on-site monitoring applications. The expense for sensor fabrication increased because of the extra photolithography and e-beam evaporation, but the cost per single sensor was still low as a result of mass production (20 sensors per batch). Also, the sensor should be applicable to other matrices such as human serum or whole blood for point-of-care measurements.

## Acknowledgments

This work was supported by funds provided by *National Institutes of Health (NIH)* Grant R21ES019255.

## References


1. Ibs K, Rink L. J Nutrition. 2003; 133:1452S. [PubMed: 12730441]
2. Heyland DK, Jones N, Cvijanovich NZ, Wong H. J Parenteral Enteral Nutrition. 2008; 32:509.
3. Williams RJP. Endeavour. 1984; 8:65. [PubMed: 6204848]
4. Wastney ME, Aamodt RL, Rumble WF, Henkin RI. Am J Physiology – Reg Integr Comp Physiol. 1986; 251:R398.
5. Brandão-Neto J, Stefan V, Mendonça BB, Bloise W, Castro AVB. Nutr Res. 1995; 15:335.
6. Cuajungco MP, Lees GJ. Neurobiol Dis. 1997; 4:137. [PubMed: 9361293]
7. Wong HR, Shanley TP, Sakthivel B, Cvijanovich N, Lin R, Allen GL, Thomas NJ, Doctor A, Kalyanaraman M, Tofil NM, Penfil S, Monaco M, Tagavilla MA, Odoms K, Dunsmore K, Barnes M, Aronow BJ. Physiol Genomics. 2007; 30:146. [PubMed: 17374846]
8. Wong H, Cvijanovich N, Lin R, Allen G, Thomas N, Willson D, Freishtat R, Anas N, Meyer K, Checchia P, Monaco M, Odom K, Shanley T. BMC Medicine. 2009; 7:34. [PubMed: 19624809]
9. Liuzzi JP, Lichten LA, Rivera S, Blanchard RK, Aydemir TB, Knutson MD, Ganz T, Cousins RJ. Proc Natl Acad Sci USA. 2005; 102:6843. [PubMed: 15863613]
10. Bhutta ZA, Nizami SQ, Isani Z. Pediatrics. 1999; 103:e42. [PubMed: 10103334]
11. Bhutta ZA, Bird SM, Black RE, Brown KH, Gardner JM, Hidayat A, Khatun F, Martorell R, Ninh NX, Penny ME, Rosado JL, Roy SK, Ruel M, Sazawal S, Shankar A. Am J Clin Nutr. 2000; 72:1516. [PubMed: 11101480]
12. Ruel MT, Rivera JA, Santizo M, Lönnerdal B, Brown KH. Pediatrics. 1997; 99:808. [PubMed: 9164774]
13. Sazawal S, Black RE, Ramsan M, Chwaya HM, Dutta A, Dhingra U, Stoltzfus RJ, Othman MK, Kabole FM. Lancet. 2007; 369:927. [PubMed: 17368154]
14. Cuajungco MP, Fagét KY. Brain Res Rev. 2003; 41:44. [PubMed: 12505647]
15. Nations SP, Boyer PJ, Love LA, Burritt MF, Butz JA, Wolfe GI, Hynan LS, Reisch J, Trivedi JR. Neurology. 2008; 71:639. [PubMed: 18525032]
16. Hotz C, Peerson JM, Brown KH. Am J Clin Nutrition. 2003; 78:756. [PubMed: 14522734]
17. Smith JC, Butrimovitz GP, Purdy WC. Clin Chem. 1979; 25:1487. [PubMed: 455691]
18. Rahman S, Waheed S. J Radioanal Nucl. 2009; 279:915.
19. Jenner GA, Longerich HP, Jackson SE, Fryer BJ. Chem Geol. 1990; 83:133.
20. Barany E, Bergdahl IA, Schütz A, Skerfving S, Oskarsson A. J Anal At Spectrom. 1997; 12:1005.
21. Wang, J. Analytical Electrochemistry. Wiley; Hoboken, NJ, USA: 2006.
22. Copeland TR, Skogerboe RK. Anal Chem. 1974; 46:1257A.
23. Opydo J. Water Air Soil Pollut. 1989; 45:43.
24. Martinotti W, Queirazza G, Guarinoni A, Mori G. Anal Chim Acta. 1995; 305:183.
25. Desmond D, Lane B, Alderman J, Hill M, Arrigan DWM, Glennon JD. Sens Actuators B, Chem. 1998; 48:409.
26. Lu T, Huang J, Sun I. Anal Chim Acta. 2002; 454:93.
27. Wang J. Electroanalysis. 2005; 17:1341.
28. Wang J, Lu J, Hocevar SB, Farias PAM, Ogorevc B. Anal Chem. 2000; 72:3218. [PubMed: 10939390]
29. Guo Z, Feng F, Hou Y, Jaffrezic-Renault N. Talanta. 2005; 65:1052. [PubMed: 18969909]
30. Kefala G, Economou A, Voulgaropoulos A, Sofoniou M. Talanta. 2003; 61:603. [PubMed: 18969224]
31. Kefala G, Economou A, Voulgaropoulos A. Analyst. 2004; 129:1082. [PubMed: 15508038]
32. Jothimuthu P, Wilson RA, Herren J, Pei X, Kang W, Daniels R, Wong H, Beyette F, Heineman WR, Papautsky I. Electroanalysis. 2013; 25:401.
33. Kruusma J, Tomčík P, Banks C, Compton R. Electroanalysis. 2004; 16:852.
34. Yue W, Bange A, Riehl BL, Johnson JM, Papautsky I, Heineman WR. Electroanalysis. 2013; 25:2261.

35. Jothimuthu P, Wilson RA, Herren J, Haynes EN, Heineman WR, Papautsky I. Biomed Microdevices. 2011; 13:695. [PubMed: 21479538]
36. Pei X, Kang W, Yue W, Bange A, Wong HR, Heineman WR, Papautsky I. Proc SPIE. 2012:8251.
37. Gharib Naseri N, Baldock SJ, Economou A, Goddard NJ, Fielden PR. Anal Bioanal Chem. 2008; 391:1283. [PubMed: 18351328]
38. Bobrowski A, Królicka A, Zarebski J. Electroanalysis. 2010; 22:1421.
39. Serrano N, Díaz-Cruz JM, Ariño C, Esteban M. Anal Bioanal Chem. 2010; 396:1365. [PubMed: 19937002]
40. Nicholson MM. Anal Chem. 1960; 32:1058.
41. Perone SP, Kretlow WJ. Anal Chem. 1965; 37:968.
42. Yue W, Riehl BL, Pantelic N, Schlueter KT, Johnson JM, Wilson RA, Guo X, King EE, Heineman WR. Electroanalysis. 2012; 24:1039.
43. CRC Handbook of Chemistry and Physics. 94. Vol. ch 6. CRC Press; Boca Raton, FL: 2013–2014.
44. Wang J, Tuzhi P. Anal Chem. 1986; 58:1787. [PubMed: 3752510]
45. Simon N, Girard H, Ballutaud D, De la Rochefoucauld E, Etcheberry A. ECS Transact. 2007; 3:59.
46. Simon N, Girard H, Manesse M, Ballutaud D, Etcheberry A. Diamond Rel Mater. 2008; 17:1371.
47. Morrison, G. Clinical Methods: The History, Physical, and Laboratory Examinations. 3. Walker, H.; Hall, W.; Hurst, J., editors. Butterworths; Boston: 1990.
48. Genuis SJ, Birkholz D, Rodushkin I, Beesoon S. Arch Environ Contam Toxicol. 2011; 61:344. [PubMed: 21057782]
49. Kruusma J, Banks CE, Nei L, Compton RG. Anal Chim Acta. 2004; 510:85.
50. Kumar MP, Mouli PC, Reddy SJ, Mohan SV. Anal Lett. 2005; 38:463.

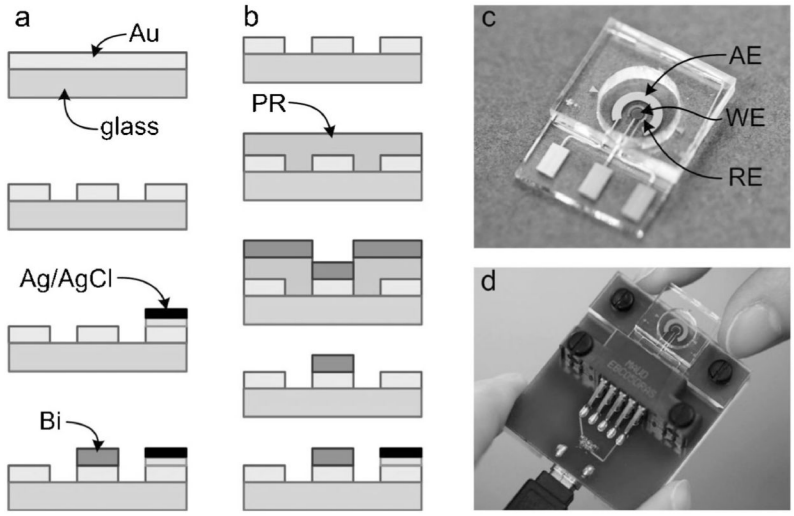


**Fig. 1.**

(a) Sequence of steps for fabrication of electrodeposited bismuth working electrode sensor includes evaporation of Au layer and its photolithographic patterning, formation of the Ag/AgCl reference electrode, and electrodeposition of Bi. (b) Sequence of steps for fabrication of evaporated bismuth working electrode sensor includes evaporation of Au layer and its photolithographic patterning, second photolithography to define sacrificial resist mask, second evaporation to deposit a thin film of bismuth, a lift-off process to pattern Bi, and formation of the Ag/AgCl reference electrode. (c) A close-up of the completed electrochemical sensor cell (AE: Au auxiliary electrode, RE: Ag/AgCl reference electrode, WE: evaporated Bi working electrode). (d) A PCB-based edge board connector interface with a mini USB cable for connection to potentiostat.

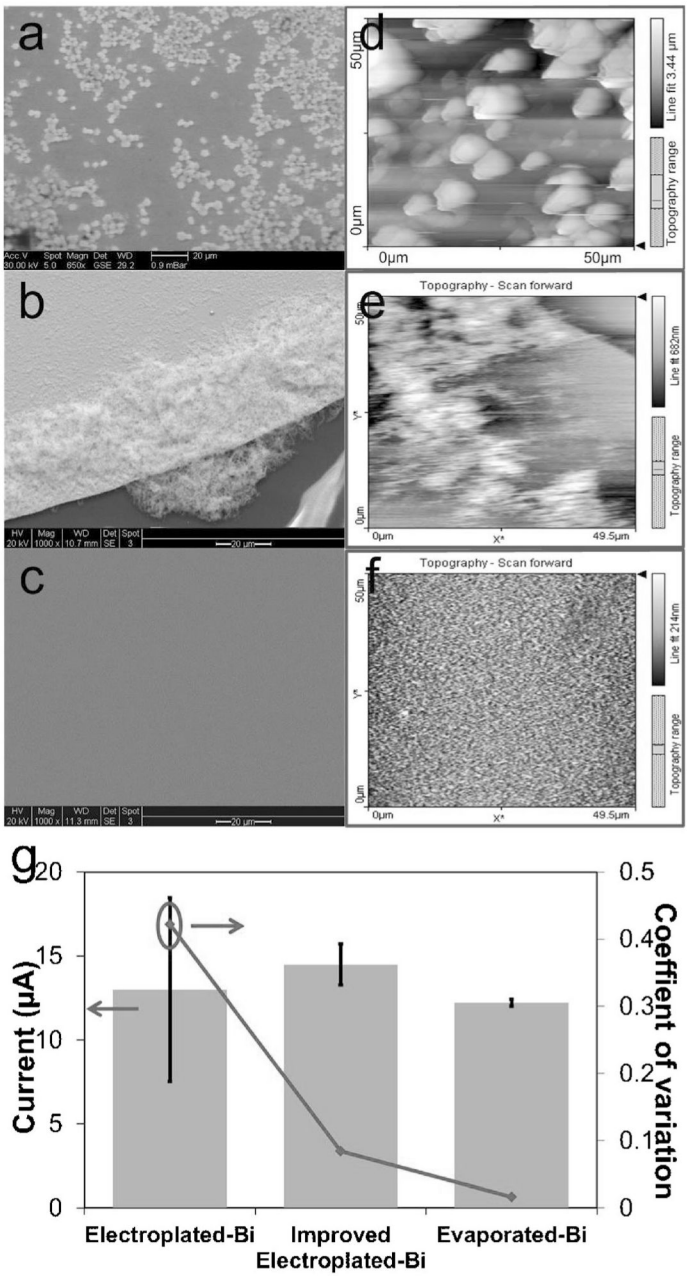


**Fig. 2.**

Comparisons of surface morphologies of electroplated bismuth working electrodes before (top) and after fabrication optimization (middle), and evaporated bismuth electrodes (bottom) : (ac) SEM images of each type of Bi WE and (d–f) AFM scans, respectively. (g) Comparisons of signal strength and reproducibility of zinc SWASV in acetate buffer using electroplated bismuth WE (left), improved electroplated Bi WE (middle), and evaporated bismuth electrodes (right).

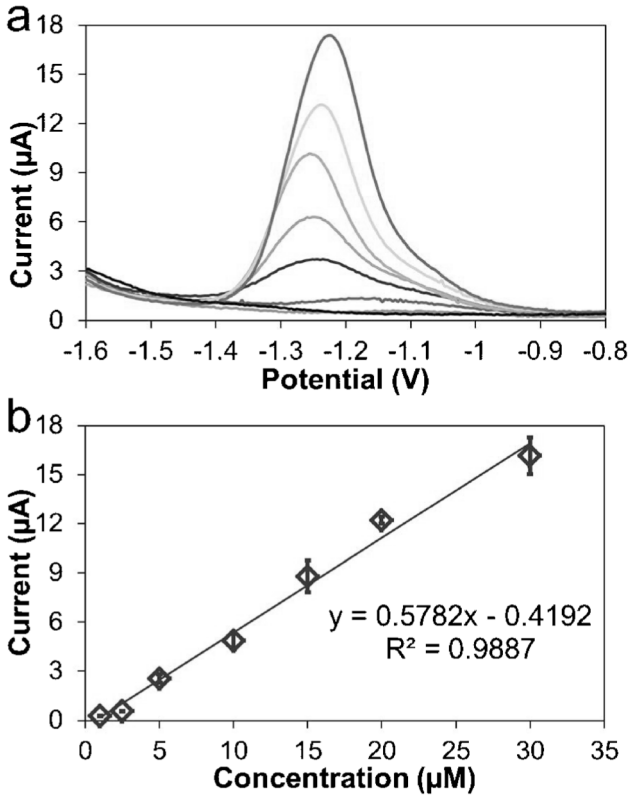


**Fig. 3.**

SWASV of zinc in pH 6 acetate buffer from 1 μM to 30 μM: (a) stripping voltammograms of Zn; (b) calibration plot. Sample volume: 100 μL; deposition potential: −1.6 V; duration: 600 s; period: 70 ms; increment: 4 mV; amplitude: 25 mV. Calculated *LOD* is 60 nM.

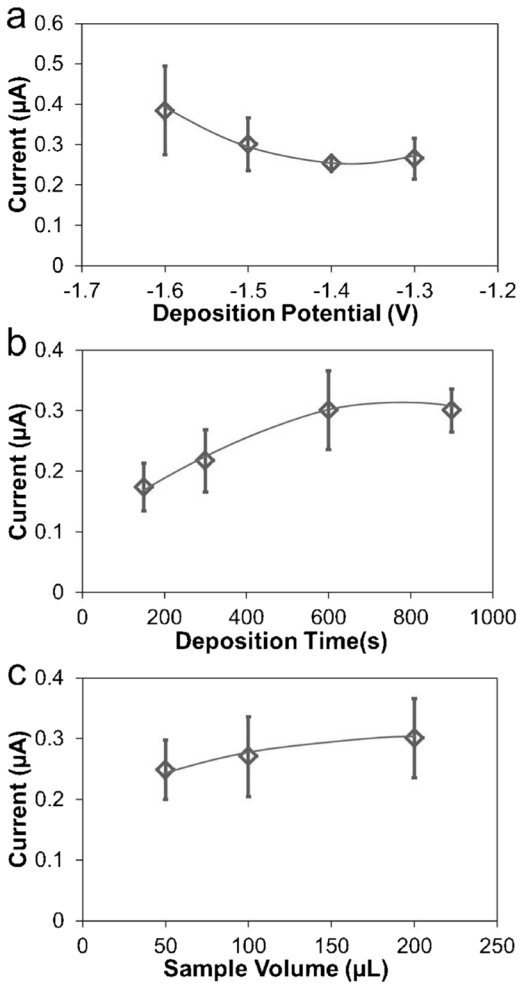


**Fig. 4.**

Optimization of SWASV conditions specifically in extracted serum diluted by pH 6 acetate buffer: (a) deposition potential; (b) deposition time; (c) sample volume.

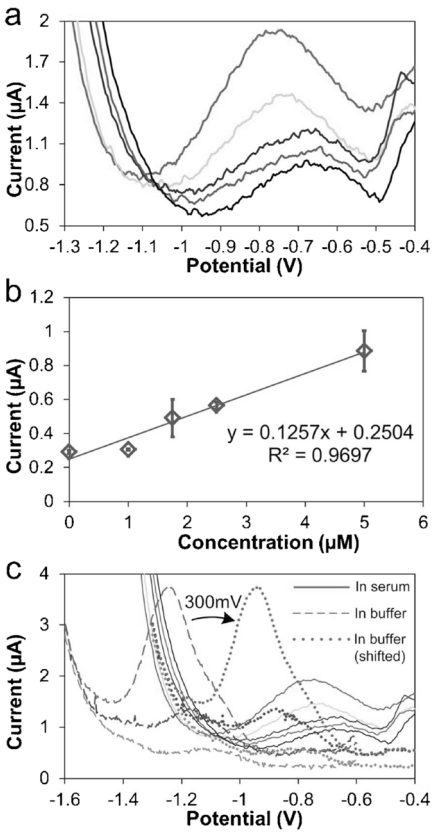


**Fig. 5.**

SWASV measurements of unknown zinc level in extracted serum: (a) voltammograms; (b) standard addition plot; (c) shifted voltammograms of Zn in acetate buffer which overlap the voltammograms of Zn in serum. Sample volume: 200 μL; deposition potential: −1.4 V; duration: 900 s; amplitude: 25 mV; period: 40 ms; increment: 4 mV. Zn concentration is calculated as 3.98 μM following standard addition approach.